Multiagent-Based Reactive Power Sharing and Control Model for Islanded Microgrids

Chen, Feixiong; Chen, Minyou; Li, Qiang; Meng, Kaikai; Guerrero, Josep M.; Abbott, Derek

Published in:
IEEE Transactions on Sustainable Energy

DOI (link to publication from Publisher):
10.1109/TSTE.2016.2539213

Publication date:
2016

Document Version
Early version, also known as pre-print

Multiagent Based Reactive Power Sharing and Control Model for Islanded Microgrids

Feixiong Chen, Minyou Chen, *Senior Member, IEEE,* Qiang Li, Kaikai Meng, Josep M. Guerrero, *Fellow, IEEE,* and Derek Abbott, *Fellow, IEEE*

***Abstract*—In islanded microgrids (MGs), the reactive power cannot be shared proportionally among distributed generators (DGs) with conventional droop control, due to the mismatch in feeder impedances. For the purpose of proportional reactive power sharing, a multiagent system (MAS) based distributed control model for droop-controlled MGs is proposed. The proposed control model consists of two layers, where the bottom layer is the electrical distribution MG, while the top layer is a communication network composed of agents. Moreover, agents on the communication network exchange the information acquired from DGs with neighbors, and calculate set points for DGs they connect to, according to the control laws. Further, a theorem is demonstrated, which yields a systematic method to derive the control laws from a given communication network. Finally, three cases are carried out to test the performance of the control model, in which the uncertainty of intermittent DGs, variations in load demands, as well as impacts of time delays are considered. The simulation results demonstrate the effectiveness of the control model in proportional reactive power sharing, and the plug and play capability of the control model is also verified.**

***Index Terms*—Microgrids (MGs), multiagent system (MAS), distributed control, reactive power sharing, plug and play.**

I. Introduction

Nowadays, world consumption of mineral resources is constantly increasing, so that the proven mineral resources reserves are progressively decreasing and even exhausted. To address these concerns, the share of renewable energy in energy consumption has been steadily growing, in the last few years [1]. And it is worth noting that the increasing trend toward renewable energy has brought forward the microgrid (MG), which facilitates the effective integration of distributed generators (DGs) into the main grid. An MG is able to operate in both islanded and grid-connected modes, as well as to transfer between these two modes seamlessly. However, the control and management of inverter-based MGs pose significant challenges, due to their low inertia, bidirectional power flows, and the uncertainty of intermittent DGs, etc [2], [3].

A popular control approach, termed centralized control, has been widely employed in MG control, and it requires all DGs to communicate with the MG central controller (MGCC), and then control decisions are broadcasted back to DGs. Therefore, the centralized control highly depends on the MGCC to process significant amounts of data, and it requires an extensive communication network to collect information globally. Moreover, there is an intrinsic disadvantage of single-point failure in centralized control, because any failures of the MGCC or its associated communication links result in the failure of the MG. On the contrary, in decentralized and distributed control, the decision making is performed based on local information, eliminating the requirement of the MGCC and extensive communication network. Therefore, the decentralized and distributed control are better suited for a large sized MG than centralized control, and the main difference between the decentralized and distributed control lies in the fact that neither interactions nor local communication network among DGs is considered in decentralized control [4], [5].

Considering the high variability of photovoltaic generators (PVs), cooperative control has been studied for distributed control of PVs [6]–[8], which has robustness against intermittency and latency on the communication network. For example, cooperative control was utilized to allow PVs to operate at the same active power utilization ratio with respect to their respective capacities [6]. And further work was carried out, which required no direct measurement of output of each PV [7]. For the case that multiple energy storage systems were organized as an MG, Xin *et al*. [8] developed an "N-1" redundant control network based on cooperative control, which satisfied both energy balance and fair utilization among energy storage systems with local measurements.

Furthermore, the multiagent system (MAS) has also been recently introduced to the area of distributed control of DGs [9]–[15]. For instance, an MAS based frequency control strategy was developed in [9], where agents exchanged information locally using an average consensus algorithm. Additionally, based on the stability of frequency, an adaptive distributed load shedding approach was investigated [10]. By combining MAS with cooperative control, Bidram *et al*. [11], [12] considered the secondary control of a droop-controlled MG as a tracking synchronization problem. Focusing on

F. Chen, M. Chen and Q. Li are with the State Key Laboratory of Power Transmission Equipment & System Security and New Technology, School of Electrical Engineering, Chongqing University, Chongqing 400044, China (e-mail: chenfeixiong87@sina.com, mchencqu@126.com and qiangli.ac@gmail.com).

K. Meng is with the Fuzhou Power Supply Company of State Grid Fujian Electric Power Company, Fujian 350000, China (e-mail: mkk20121102067@163.com).

J. M. Guerrero is with the Department of Energy Technology, Aalborg University, 9220 Aalborg East, Denmark (Tel: +45 2037 8262; Fax: +45 9815 1411; e-mail: joz@et.aau.dk).

D. Abbott is with the School of Electrical and Electronic Engineering, University of Adelaide, Adelaide, SA 5005, Australia (e-mail: derek.abbott@adelaide.edu.au).

Manuscript received XX, 2015; revised XX, 2016.

distributed energy storages in an MG, an MAS based dynamic control strategy was demonstrated in [13], which allowed energy storages operate at a common energy level. In addition, a hierarchical MAS based energy management was developed to manage and optimize the MG operations [14]. And in our recent work [15], an agent-based control model for islanded MGs was proposed, which guaranteed the demand and supply balance, as well as the stability of frequency and voltage.

Moreover, the droop control has long been applied to decentralized control of islanded MGs, which requires no intercommunication among DGs. As is known, the accurate active power sharing is obtained easily by droop control, but due to the mismatch in feeder impedances between DGs, the conventional droop control achieves poor reactive power sharing among DGs, even with proportional droop coefficients [16], [17]. In other words, conventional droop control cannot distribute generation responsibility among DGs with respect to their respective power ratings, which may possibly result in a number of DGs being overload. Consequently, with the aim of proportional reactive power sharing, Guerrero *et al*. [18], [19] formulated the adaptive virtual output impedance. Further, the strategy based on static droop characteristics and transient droop function was developed [20]. Additionally, the method of optimum droop parameter settings for reactive power sharing was provided [21]. And based on current sensing and adaptive virtual impedance, Zhu *et al*. [22] developed a wireless reactive power sharing strategy.

It is worth noting that the introduction of communication network to droop control enhances the accuracy of reactive power sharing [23]–[34]. In [23], [24], a distributed strategy for secondary control and proportional reactive power sharing was investigated, where each DG required information of all other DGs in the MG. Further, the improvements were carried out in [25], [26], where each DG required information exchange with only a few neighboring DGs. Based on the work carried out in [11], [12], further work was performed to achieve power sharing among DGs [27]. In addition, the application of distributed finite-time control to distributed secondary control and power sharing was explored [28]. Considering the conflicting goals of voltage regulation and reactive power sharing, a distributed averaging proportional integral controller for secondary control was presented in [29]. With the consideration of dynamical models of PVs, battery energy storage systems, and plug-in hybrid vehicles, a nonlinear distributed controller for power sharing was developed [30]. Moreover, a distributed voltage control and reactive power sharing strategy was presented in [31], which was based on weighted average consensus protocol, and corresponding rigorous mathematical analysis was given. And Han *et al*. [32] improved the sharing accuracy by means of sharing error reduction and voltage recovery. In [33], a consensus-based power sharing method was developed, which was effective for alleviating the effects of non-ideal line impedances. Moreover, a distributed reactive power sharing approach was formulated in [34], where consensus control was utilized to adaptively adjust the virtual impedances.

On the other hand, DC MGs are emerging and they have attracted much attention, for DC MGs have several potential advantages over AC MGs, including simpler models and reduced conversion losses, etc [35]. With regard to distributed voltage control and power sharing in DC MGs, several distributed approaches based on information of average voltage and current of neighboring DGs were explored [36]–[39]. In [36], the control loop based on the average total current was developed for power sharing. Nasirian *et al*. [37] focused on a distributed primary and secondary controller for DC MGs, which employed a sparse communication network for data exchange among DGs. Based on dynamic consensus algorithm, a distributed hierarchical control approach for accurate current sharing and voltage restoration was proposed [38]. Additionally, an MAS based supervisory control was developed for power sharing and optimal power dispatch [39], where the average consensus algorithm was adopted for synchronous communication.

It is worth noting that in the existing methods [23]–[26], [29], [36]–[39], with the aim of power sharing, each DG collects the information i.e., the voltages, currents and power outputs of neighboring DGs using local communication network, and then the averages are calculated and used for adjusting the operation states of DGs, termed here the average methods. Motivated by the average methods discussed in the literature, in this paper, a two-layer MAS based reactive power sharing and control model is presented for a droop-controlled MG, where the bottom layer is the electrical distribution MG, while the top layer is an MAS communication network composed of agents. Moreover, the agents can collect the information of corresponding DGs, i.e., reactive power outputs, by means of communication links between two layers, and then they exchange the information acquired with their neighboring agents on the communication network. Furthermore, a theorem is proved, which provides a systematic method to derive the control laws from a given communication network. And in terms of acquired information and the control laws, the average reactive power outputs of neighboring controllable DGs can be calculated, i.e., the reference reactive power outputs. After that, the references are sent to DGs, to adjust their reactive power outputs. Finally, simulation cases are performed to verify the feasibility, as well as plug and play capability of the control model. According to the results, it can be found that the proportional power sharing is achieved, when the control laws are used, moreover, the plug out and plug in of the DG and agent do not affect the performance of the control model.

Furthermore, compared to existing methods, the salient features of the proposed control model are (i) a theorem is proved, which yields a systematic method for deriving the control laws from a given communication network, and then the reactive power references can be calculated conveniently in terms of the control laws, therefore making it more suitable for practical applications; (ii) the proposed control model has the capability of plug and play, which is not extensively discussed in the existing methods; (iii) the proposed control model is fully distributed, and each unit simply requires the information of reactive power outputs of its neighboring DGs, by means of a sparse communication network, which reduces

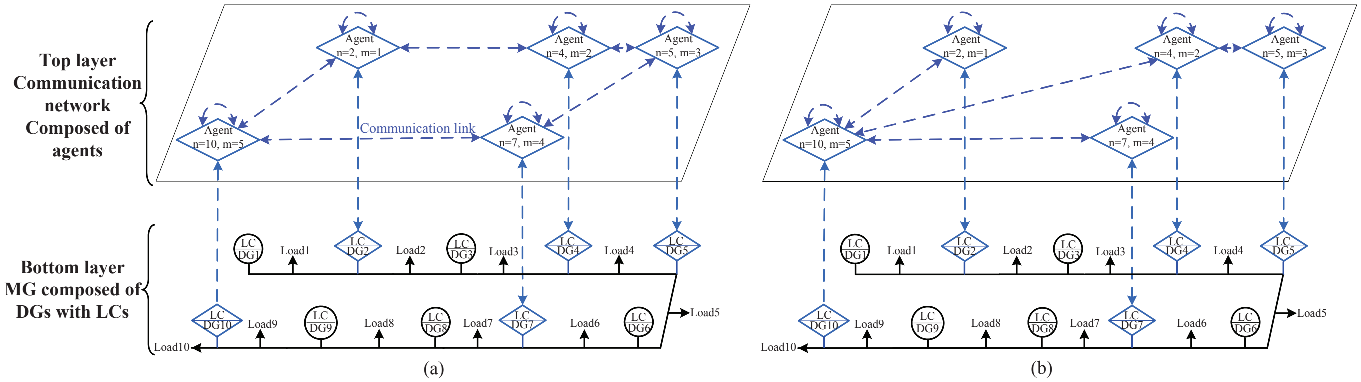

Fig. 1. The two-layer control model for islanded MGs. (a) Network 1: the ring communication network. (b) Network 2: the radial communication network. For the same MG, two different communication networks are established and used.

the communication cost.

The rest of the paper is organized as follows. In Section II, the MAS based control model for islanded MGs is formulated and described in detail. And in Section III, a theorem is demonstrated for deriving the control laws from a given communication network. Later, the structure and parameters of the islanded MG are introduced and listed in Section IV. In Section V, three cases with different settings are carried out to test the performance of the control model. Finally, Section VI concludes the paper.

II. Control Model for Islanded MGs

A. Control Model

In this paper, a two-layer control model is established, where the bottom layer is the electrical distribution MG, which consists of DGs, local controllers (LCs) and loads, while the top layer is an MAS communication network composed of agents, as shown in Fig. 1. Generally speaking, there are two types of DGs in an MG, i.e., *intermittent* and *controllable*, according to the characteristics of the output power [40]. For clarity, in the proposed control model, the intermittent DGs are indicated by circles, while controllable DGs and corresponding agents are illustrated by diamonds, as shown in Fig. 1. And it can be found in Fig. 1 that there exist bidirectional communication links between two layers and among agents, and agents have self loops. Further, the arrows on dashed lines on the communication network, and between two layers indicate the information transfer directions.

Therefore, by means of communication links, agents can collect the information of controllable DGs they connect to, i.e., the reactive power output, and then agents exchange the information acquired with their neighbors on the communication network. After that, the set points of controllable DGs can be calculated by agents, in terms of acquired information and control laws. Thereafter, the set points are sent to controllable DGs to adjust their reactive power outputs.

B. MAS Based Communication Network

In this paper, the MAS communication network is modeled by a directed graph $G(V, E)$, where V is the set of nodes or agents, and E is the set of edges or communication links. In order to describe the relationships between m agents, an $m \times m$ adjacency matrix A is used, where the entry $a_{ij} = 1$ means there is a communication link from Agent$_i$ to Agent$_j$, otherwise $a_{ij} = 0$. Also, an $m \times m$ and diagonal outdegree matrix D is employed to count the number of outgoing communication links of an agent, known as the outdegree d_{ii} of Agent$_i$. Moreover, the parameter k is defined as $k = \max(d_{11}, \cdots, d_{ii}, \cdots, d_{mm})$. Finally, $(k{\cdot}I)^{-1}$ is the inverse matrix of $k \cdot I$, and I is an $m \times m$ identity matrix.

It is should be emphasized that the topology of the MAS communication network is independent of the structure of the MG. In other words, it is not required that the topology of the communication network is identical to that of the MG. Therefore, many possible communication networks can be considered for a given MG, but each communication network possesses a set of control laws. In this paper, two communication networks with different topologies, network 1 and 2, are designed for the same MG, as shown in Fig. 1. Moreover, the communication network must be connected, i.e., there are no isolated agents on the communication network, for connected communication network allows communication among agents.

Furthermore, if the topology of the communication network is identical to that of the MG, the power line communication is a feasible manner to transmit information among agents. In the case that the topology of the communication network is different from that of the MG, other mature communication technologies are available, e.g., TCP/IP communication, optical fiber communication.

III. Distributed Control Laws for Reactive Power Sharing

For the purpose of reactive power sharing, in this section, a theorem is proved for deriving the control laws from a given communication network. And then in terms of the control laws, agents regulate the reactive power outputs of controllable DGs to which they connect, to realize the proportional power sharing.

First, the ratios of outputs of controllable DGs to their respective power ratings are defined. And suppose for the ith controllable DG, the active and reactive power ratios can be

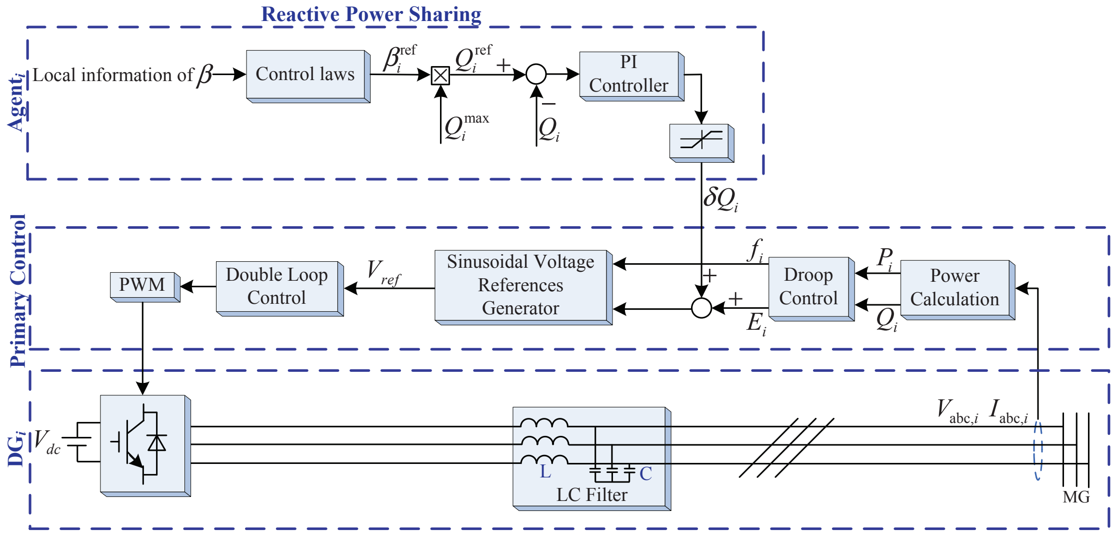

Fig. 2. Schematic of distributed reactive power sharing.

calculated

$$\begin{cases} \alpha_i = P_i / P_i^{\max}, \\ \beta_i = Q_i / Q_i^{\max}, \end{cases} \tag{1}$$

where α_i and β_i denote active and reactive power ratios, P_i, Q_i are active and reactive power outputs of controllable DG$_i$, and $P_i^{\max}$, $Q_i^{\max}$ are active and reactive power ratings of DG$_i$, respectively.

As discussed in Section II, agents can collect the information of reactive power outputs of controllable DGs they connect to. Therefore, receiving the information, the reactive power ratios can be calculated by agents in terms of (1), and then agents exchange the information of reactive power ratios with their neighbors on the communication network. Thereafter, in terms of the control laws and acquired information, the average reactive power ratios of neighboring controllable DGs can be calculated, i.e., the reference reactive power ratios, as illustrated in Fig. 2. Consequently, a theorem is proved, which provides a systemic method to derive the control laws for a given communication network.

Theorem: Let $G(V, E)$ be a directed communication network with m agents, if agents calculate the reference reactive power ratios in terms of (2), and apply the results to regulate reactive power outputs of controllable DGs to which they connect, then the proportional reactive power sharing among controllable DGs is guaranteed, namely, $\beta_1 = \cdots = \beta_i \cdots = \beta_m$,

$$\beta^{\text{ref}} = (k \cdot I)^{-1} \cdot [A + (k \cdot I - D)] \cdot \beta, \tag{2}$$

where $\beta^{\text{ref}} = (\beta_i^{\text{ref}})_{m\times 1}$, $\beta = (\beta_i)_{m\times 1}$.

Proof: First, $k \cdot I - D$ is calculated

$$k \cdot I - D = \begin{bmatrix} k - d_{11} & & & & \\ & \ddots & & & \\ & & k - d_{ii} & & \\ & & & \ddots & \\ & & & & k - d_{mm} \end{bmatrix}. \tag{3}$$

Therefore, $A + (k \cdot I - D)$

$$= \begin{bmatrix} a_{11} + k - d_{11} & \cdots & a_{1i} & \cdots & a_{1m} \\ \vdots & \ddots & \vdots & \vdots & \vdots \\ a_{i1} & \cdots & a_{ii} + k - d_{ii} & \cdots & a_{im} \\ \vdots & \vdots & \vdots & \ddots & \vdots \\ a_{m1} & \cdots & a_{mi} & \cdots & a_{mm} + k - d_{mm} \end{bmatrix}. \tag{4}$$

Then, in terms of (2), we can obtain the reference reactive power ratios

$$\begin{aligned} \beta^{\text{ref}} &= (k \cdot I)^{-1} \cdot [A + (k \cdot I - D)] \cdot \beta \\ &= \frac{1}{k} \begin{bmatrix} 1 & & & & \\ & \ddots & & & \\ & & 1 & & \\ & & & \ddots & \\ & & & & 1 \end{bmatrix} \\ &\cdot \begin{bmatrix} a_{11} + k - d_{11} & \cdots & a_{1i} & \cdots & a_{1m} \\ \vdots & \ddots & \vdots & \vdots & \vdots \\ a_{i1} & \cdots & a_{ii} + k - d_{ii} & \cdots & a_{im} \\ \vdots & \vdots & \vdots & \ddots & \vdots \\ a_{m1} & \cdots & a_{mi} & \cdots & a_{mm} + k - d_{mm} \end{bmatrix} \begin{bmatrix} \beta_1 \\ \vdots \\ \beta_i \\ \vdots \\ \beta_m \end{bmatrix}. \end{aligned} \tag{5}$$

According to (5), the concrete formulas for calculating reference reactive power ratios can be obtained

$$\begin{cases} \beta_1^{\text{ref}} = \frac{1}{k}[\beta_1 \cdot (a_{11} + k - d_{11}) + \cdots + \beta_i \cdot a_{1i} + \cdots + \beta_m \cdot a_{1m}], \\ \quad \vdots \\ \beta_i^{\text{ref}} = \frac{1}{k}[\beta_1 \cdot a_{i1} + \cdots + \beta_i \cdot (a_{ii} + k - d_{ii}) + \cdots + \beta_m \cdot a_{im}], \\ \quad \vdots \\ \beta_m^{\text{ref}} = \frac{1}{k}[\beta_1 \cdot a_{m1} + \cdots + \beta_i \cdot a_{mi} + \cdots + \beta_m \cdot (a_{mm} + k - d_{mm})]. \end{cases} \tag{6}$$

Consequently, the reference reactive power outputs $Q^{\text{ref}} =$

$(Q_i^{\text{ref}})_{m\times 1}$ for controllable DGs can be calculated

$$\begin{cases} Q_1^{\text{ref}} = \beta_1^{\text{ref}} \cdot Q_1^{\max}, \\ \vdots \\ Q_i^{\text{ref}} = \beta_i^{\text{ref}} \cdot Q_i^{\max}, \\ \vdots \\ Q_m^{\text{ref}} = \beta_m^{\text{ref}} \cdot Q_m^{\max}. \end{cases} \tag{7}$$

It is worth noting that the proportional reactive power sharing is based on reactive power balance, which is ensured by primary droop control. And in this paper, we employ PI controllers to drive reactive power outputs of controllable DGs, $Q = (Q_i)_{m\times 1}$ converges to $Q^{\text{ref}} = (Q_i^{\text{ref}})_{m\times 1}$ gradually [23]. Meanwhile, the reactive power ratios, $\beta = (\beta_i)_{m\times 1}$ also approaches $\beta^{\text{ref}} = (\beta_i^{\text{ref}})_{m\times 1}$. Therefore, in the steady state, from the reactive power sharing schematic in Fig. 2, we have the following expressions

$$\begin{cases} \sum_{i=1}^{m} \delta Q_i = \sum_{i=1}^{m} (Q_i^{\text{ref}} - Q_i) = 0, \\ \sum_{i=1}^{m} Q_i^{\text{ref}} = \sum_{i=1}^{m} Q_i, \\ \sum_{i=1}^{m} Q_i^{\max} \cdot \beta_i^{\text{ref}} = \sum_{i=1}^{m} Q_i^{\max} \cdot \beta_i. \end{cases} \tag{8}$$

According to (8), the equations in (9) are satisfied in the steady state

$$\begin{cases} \beta_1^{\text{ref}} = \beta_1, \\ \vdots \\ \beta_i^{\text{ref}} = \beta_i, \\ \vdots \\ \beta_m^{\text{ref}} = \beta_m. \end{cases} \tag{9}$$

Therefore, applying conditions (9) to (6), we have the following equation set

$$\begin{cases} \frac{1}{k}[\beta_1 \cdot (a_{11} + k - d_{11}) + \cdots + \beta_i \cdot a_{1i} + \cdots + \beta_m \cdot a_{1m}] = \beta_1, \\ \quad \vdots \\ \frac{1}{k}[\beta_1 \cdot a_{i1} + \cdots + \beta_i \cdot (a_{ii} + k - d_{ii}) + \cdots + \beta_m \cdot a_{im}] = \beta_i, \\ \quad \vdots \\ \frac{1}{k}[\beta_1 \cdot a_{m1} + \cdots + \beta_i \cdot a_{mi} + \cdots + \beta_m \cdot (a_{mm} + k - d_{mm})] = \beta_m. \end{cases} \tag{10}$$

Moreover, the expressions in (10) can be simplified as

$$\begin{cases} \beta_1 \cdot (a_{11} - d_{11}) + \cdots + \beta_i \cdot a_{1i} + \cdots + \beta_m \cdot a_{1m} = 0, \\ \quad \vdots \\ \beta_1 \cdot a_{i1} + \cdots + \beta_i \cdot (a_{ii} - d_{ii}) + \cdots + \beta_m \cdot a_{im} = 0, \\ \quad \vdots \\ \beta_1 \cdot a_{m1} + \cdots + \beta_i \cdot a_{mi} + \cdots + \beta_m \cdot (a_{mm} - d_{mm}) = 0. \end{cases} \tag{11}$$

And the determinant for the coefficient matrix B of (11) is obtained as follows,

$$|B| = \begin{vmatrix} a_{11} - d_{11} & \cdots & a_{1i} & \cdots & a_{1m} \\ \vdots & \ddots & \vdots & \vdots & \vdots \\ a_{i1} & \cdots & a_{ii} - d_{ii} & \cdots & a_{im} \\ \vdots & \vdots & \vdots & \ddots & \vdots \\ a_{m1} & \cdots & a_{mi} & \cdots & a_{mm} - d_{mm} \end{vmatrix}. \tag{12}$$

Furthermore, according to graph theory, for the i-th row of the adjacency matrix A, the sum of all elements in the row vector equals the outdegree of Agent$_i$, therefore, the following equation is obtained

$$\sum_{j=1}^{m} a_{ij} = d_{ii}. \tag{13}$$

Applying condition (13) to (12), it yields the following equation

$$|B| = 0. \tag{14}$$

In terms of (14), there exist non-zero solutions for the equation set in (11). In order to obtain non-zero solutions for (11), the rank of the coefficient matrix B is calculated first, which is equal to that of B^T. In other words, we have

$$R(B) = R(B^T) = R \begin{bmatrix} a_{11} - d_{11} & \cdots & a_{i1} & \cdots & a_{m1} \\ \vdots & \ddots & \vdots & \vdots & \vdots \\ a_{1i} & \cdots & a_{ii} - d_{ii} & \cdots & a_{mi} \\ \vdots & \vdots & \vdots & \ddots & \vdots \\ a_{1m} & \cdots & a_{im} & \cdots & a_{mm} - d_{mm} \end{bmatrix}. \tag{15}$$

Applying condition (13) to (15), the rank of the coefficient matrix B is obtained

$$R(B) = R(B^T) = m - 1. \tag{16}$$

And the equation (16) denotes that the basic solutions for (11) simply have one solution vector. Moreover, we know that $m \times 1$ unit column vector is one of non-zero solutions for (11), therefore, the $m \times 1$ unit column vector is the basic solution for (11). Finally, we obtain general solutions for equation set in (11) as follows,

$$\begin{bmatrix} \beta_1 \\ \vdots \\ \beta_i \\ \vdots \\ \beta_m \end{bmatrix} = k \cdot \begin{bmatrix} 1 \\ \vdots \\ 1 \\ \vdots \\ 1 \end{bmatrix}. \tag{17}$$

where $0 \leq k \leq 1$.

Therefore,

$$\beta_1 = \cdots = \beta_i \cdots = \beta_m = k. \tag{18}$$

That is, the theorem is proved. ■

IV. Microgrid System Architecture

In this section, the setup of the islanded MG under test is introduced first. Later, in terms of the theorem, two sets of control laws are derived from two different communication networks shown in Fig. 1.

A. MG Structure

Fig. 3 illustrates the single-line diagram of the MG test system, which is established in MATLAB/Simulink, and used to verify the effectiveness of the proposed control model. The MG is composed of 10 DGs, namely $n = 10$, and the specifications of loads and capacities of DGs are listed in Fig. 3. Here, DG_1 and DG_3 are PVs, while DG_6, DG_8 and DG_9 are permanent magnet synchronous generator (PMSG) based wind turbines, all of which work in maximum power point tracking (MPPT) control mode, and they produce no reactive power, that is $Q_1 = Q_3 = Q_6 = Q_8 = Q_9 = 0$. Additionally, the dc-links of controllable DGs, e.g., micro gas turbine, are modeled as constant dc voltage sources $V_{\rm dc}$, and we assume that the voltage variations of dc-links are well regulated. Furthermore, controllable DGs are all operate in the manner of droop control.

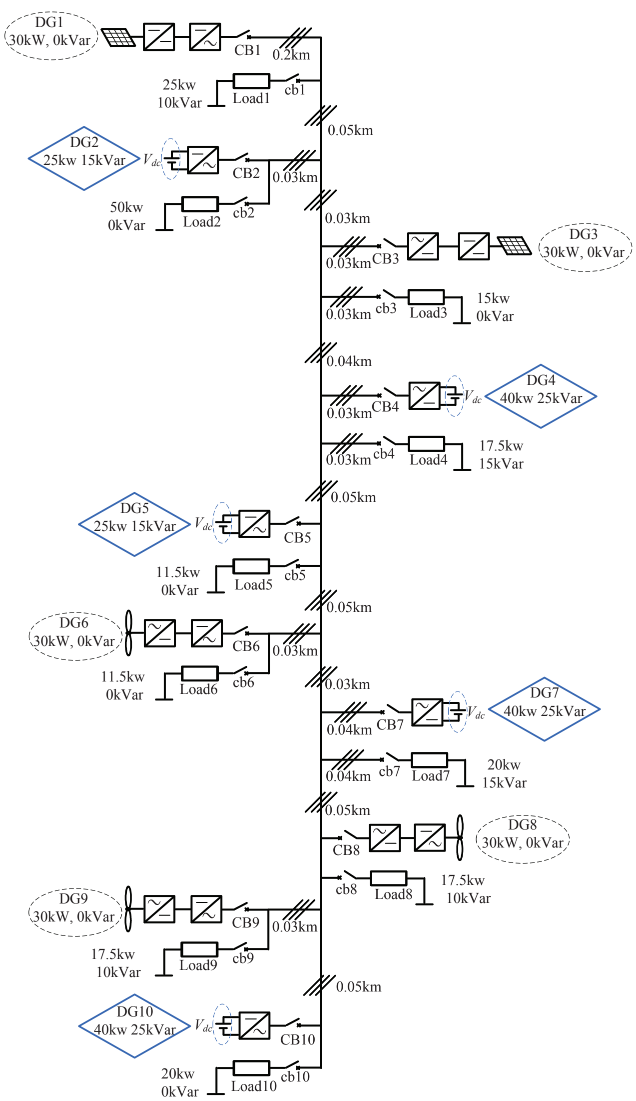

Fig. 3. Schematic diagram of an islanded MG with radial structure.

As discussed in Section III, PI controllers are adopted to drive reactive power outputs of controllable DGs to references. Therefore, according to critical ratio method, the proportional gains of PI controllers are reasonably chosen so that controllers respond quickly to changes, while the stability of the MG is guaranteed. The integral gains, on the other hand, ought to be set high enough to eliminate steady state errors, and avoid excessive overshoots. Moreover, the saturation limits of PI controllers ensure that the reactive power correction term δQ does not affect the stability of the MG. In addition, specifications of the control model are summarized in Table I.

TABLE I
PARAMETERS OF THE CONTROL MODEL

	MG Setup	
V_{dc}	DC voltage	800 V
C	Filter capacitance	4 mH
L	Filter inductance	8 μF
	Primary droop Control	
$m2$, $m5$	$P-\omega$ coefficients for DG_2, DG_5	1.01e-4 W/rd.s
$m4$, $m7$, $m10$	$P-\omega$ coefficients for DG_4, DG_7, DG_{10}	6.28e-5 W/rd.s
$n2$, $n5$	$Q-E$ coefficients for DG_2, DG_5	9.42e-4 VAr/V
$n4$, $n7$, $n10$	$Q-E$ coefficients for DG_4, DG_7, DG_{10}	5.65e-4 VAr/V
	Reactive Power Sharing	
$k_{\rm PQ}$	Proportional gain	0.000002 VAr/V
$k_{\rm iQ}$	Integral gain	0.005 VAr/Vs
upper, lower	Saturation limits of PI controllers	5, -5

Furthermore, in order to remove deviations in voltage and frequency, the distributed secondary control is carried out to recover voltage and frequency to their nominal values of 380 V and 50 Hz [41], respectively. And the distributed secondary control is elaborated in [23], hence it is not discussed further here. In the MG, the line impedance is also considered, which is set at $0.642 + j0.083\ \Omega$/km.

Meanwhile, the MG system initially works in a balanced state, and sample time is 1ms. And it is worth noting that the proposed control model can also be implemented with asynchronous communication, where no communication is needed, if the data remains unchanged. However, if updated data is received, agents will recalculate the set points for controllable DGs. In this manner, the sample time can be longer.

B. Control Laws from Given Communication Networks

According to the theorem, a set of control laws can be derived from communication network 1 and network 2, respectively, named here the control laws I and II. In order to obtain control laws I, the adjacency matrix A_1, outdegree matrix D_1, and the parameter k_1 for communication network 1 can be obtained as follows,

$$A_1 = \begin{bmatrix} 1 & 1 & 0 & 0 & 1 \\ 1 & 1 & 1 & 0 & 0 \\ 0 & 1 & 1 & 1 & 0 \\ 0 & 0 & 1 & 1 & 1 \\ 1 & 0 & 0 & 1 & 1 \end{bmatrix}, D_1 = k_1 \cdot I = \begin{bmatrix} 3 & 0 & 0 & 0 & 0 \\ 0 & 3 & 0 & 0 & 0 \\ 0 & 0 & 3 & 0 & 0 \\ 0 & 0 & 0 & 3 & 0 \\ 0 & 0 & 0 & 0 & 3 \end{bmatrix}. \tag{19}$$

Therefore,

$$(k_1 \cdot I)^{-1} \cdot [A_1 + (k_1 \cdot I - D_1)] = \frac{1}{3} \begin{bmatrix} 1 & 1 & 0 & 0 & 1 \\ 1 & 1 & 1 & 0 & 0 \\ 0 & 1 & 1 & 1 & 0 \\ 0 & 0 & 1 & 1 & 1 \\ 1 & 0 & 0 & 1 & 1 \end{bmatrix}. \tag{20}$$

And then in terms of the theorem, we can obtain the control laws I for calculating reference reactive power ratios, which take the following forms,

$$\beta_1^{\text{ref}} = \frac{1}{3}\beta_1 + \frac{1}{3}\beta_2 + \frac{1}{3}\beta_5, \tag{21}$$

$$\beta_2^{\text{ref}} = \frac{1}{3}\beta_1 + \frac{1}{3}\beta_2 + \frac{1}{3}\beta_3, \tag{22}$$

$$\beta_3^{\text{ref}} = \frac{1}{3}\beta_2 + \frac{1}{3}\beta_3 + \frac{1}{3}\beta_4, \tag{23}$$

$$\beta_4^{\text{ref}} = \frac{1}{3}\beta_3 + \frac{1}{3}\beta_4 + \frac{1}{3}\beta_5, \tag{24}$$

$$\beta_5^{\text{ref}} = \frac{1}{3}\beta_1 + \frac{1}{3}\beta_4 + \frac{1}{3}\beta_5. \tag{25}$$

Consequently, the reference reactive power outputs for controllable DGs, DG_2, DG_4, DG_5, DG_7, DG_{10} can be calculated

$$Q_2^{\text{ref}} = \beta_1^{\text{ref}} \cdot Q_2^{\max}, \tag{26}$$

$$Q_4^{\text{ref}} = \beta_2^{\text{ref}} \cdot Q_4^{\max}, \tag{27}$$

$$Q_5^{\text{ref}} = \beta_3^{\text{ref}} \cdot Q_5^{\max}, \tag{28}$$

$$Q_7^{\text{ref}} = \beta_4^{\text{ref}} \cdot Q_7^{\max}, \tag{29}$$

$$Q_{10}^{\text{ref}} = \beta_5^{\text{ref}} \cdot Q_{10}^{\max}. \tag{30}$$

Similarly, the control laws II for communication network 2 are obtained, after A_2, D_2, and $k_2 \cdot I$ are calculated

$$A_2 = \begin{bmatrix} 1 & 0 & 0 & 0 & 1 \\ 0 & 1 & 1 & 0 & 1 \\ 0 & 1 & 1 & 0 & 0 \\ 0 & 0 & 0 & 1 & 1 \\ 1 & 1 & 0 & 1 & 1 \end{bmatrix}, D_2 = \begin{bmatrix} 2 & 0 & 0 & 0 & 0 \\ 0 & 3 & 0 & 0 & 0 \\ 0 & 0 & 2 & 0 & 0 \\ 0 & 0 & 0 & 2 & 0 \\ 0 & 0 & 0 & 0 & 4 \end{bmatrix}, \tag{31}$$

$$k_2 \cdot I = \begin{bmatrix} 4 & 0 & 0 & 0 & 0 \\ 0 & 4 & 0 & 0 & 0 \\ 0 & 0 & 4 & 0 & 0 \\ 0 & 0 & 0 & 4 & 0 \\ 0 & 0 & 0 & 0 & 4 \end{bmatrix}. \tag{32}$$

Hence, in terms of the theorem, the control laws II for calculating reference reactive power ratios are obtained

$$\beta_1^{\text{ref}} = \frac{3}{4}\beta_1 + \frac{1}{4}\beta_5, \tag{33}$$

$$\beta_2^{\text{ref}} = \frac{1}{2}\beta_2 + \frac{1}{4}\beta_3 + \frac{1}{4}\beta_5, \tag{34}$$

$$\beta_3^{\text{ref}} = \frac{1}{4}\beta_2 + \frac{3}{4}\beta_3, \tag{35}$$

$$\beta_4^{\text{ref}} = \frac{3}{4}\beta_4 + \frac{1}{4}\beta_5, \tag{36}$$

$$\beta_5^{\text{ref}} = \frac{1}{4}\beta_1 + \frac{1}{4}\beta_2 + \frac{1}{4}\beta_4 + \frac{1}{4}\beta_5. \tag{37}$$

V. Results

In this section, three cases are designed to evaluate the performance of the control model, when both active power outputs of intermittent DGs and load demands change at the same time. Case 1 focuses on the effectiveness of the control model in reactive power sharing. Further, the impacts of time delays on reactive power sharing are investigated in case 2.

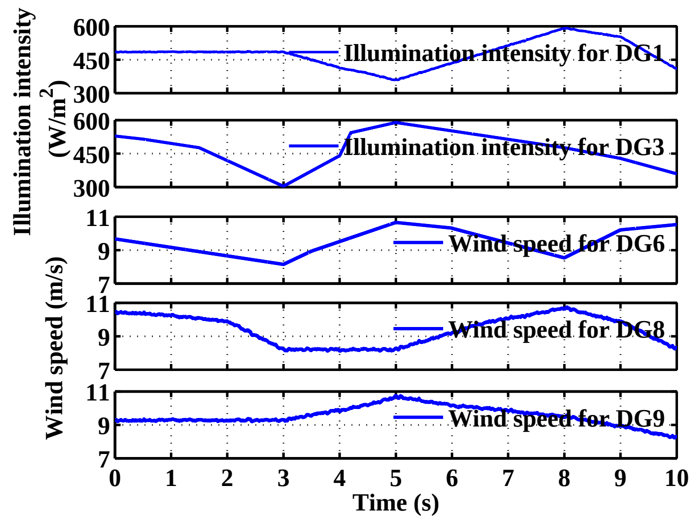

(a) the illumination intensity and wind speed.

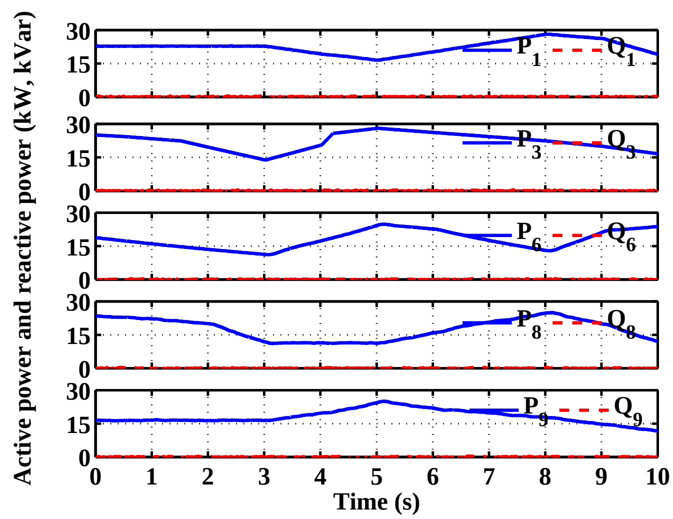

(b) power outputs of intermittent DGs.

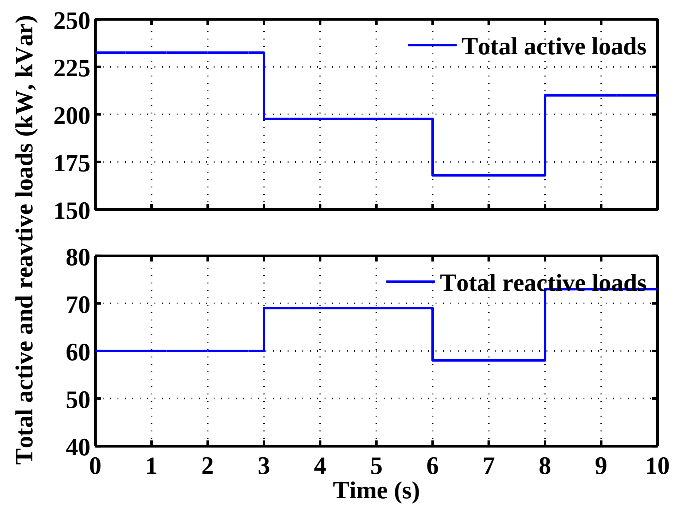

(c) load changes over time.

Fig. 4. Power outputs of intermittent DGs and load demands in the MG.

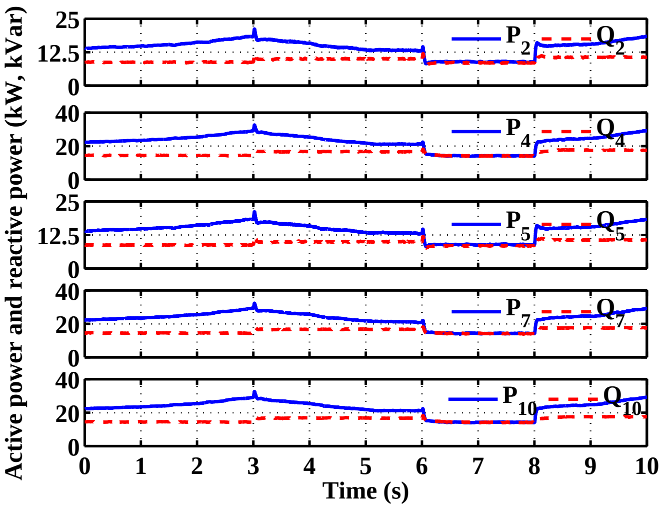

(a) power outputs of controllable DGs.

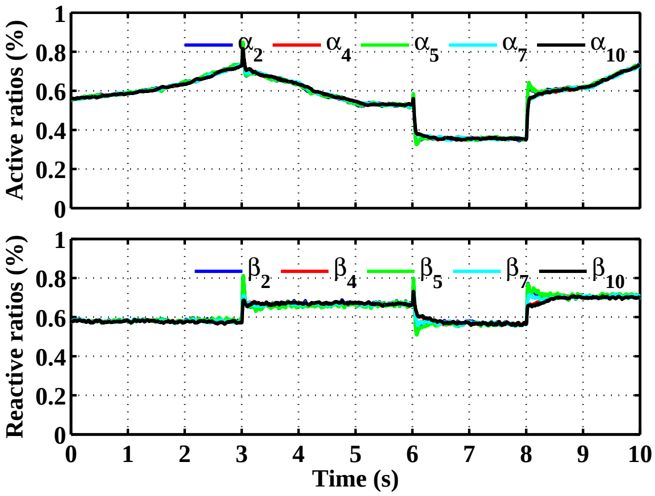

(b) power ratios of controllable DGs.

Fig. 5. Case 1: Simulation results under the control laws I, when both the environmental conditions and load demands change simultaneously.

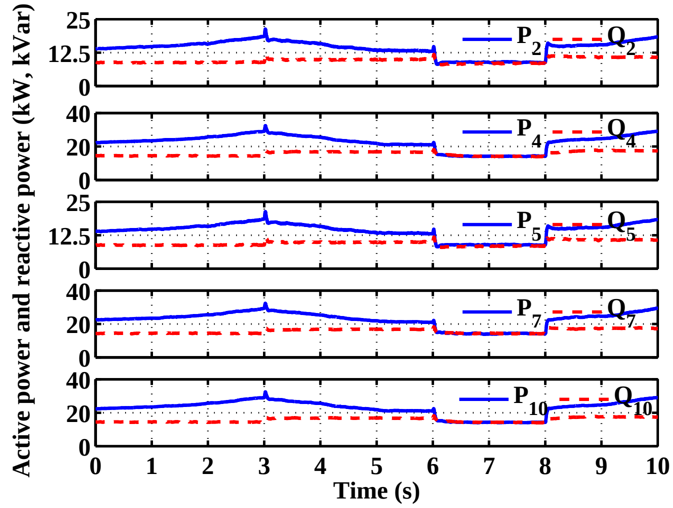

(a) power outputs of controllable DGs.

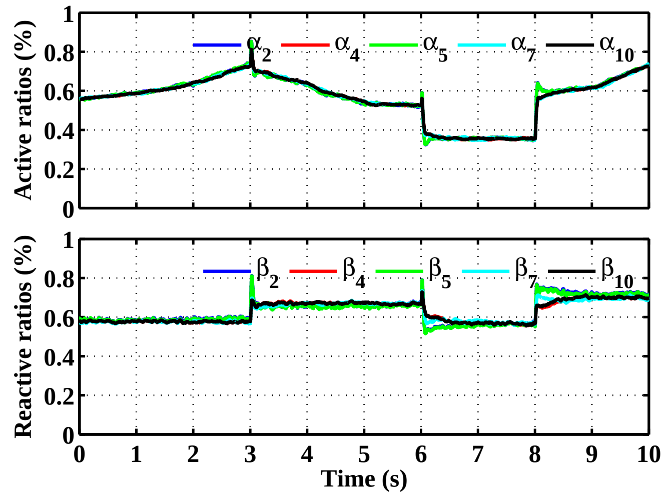

(b) power ratios of controllable DGs.

Fig. 6. Case 1: Simulation results under the control laws II, when both the environmental conditions and load demands change simultaneously.

Later, in case 3, the capability of plug and play is verified. Finally, the results are discussed and explained in detail.

For these three cases, the active power outputs of intermittent DG_1, DG_3, DG_6, DG_8 and DG_9 change between 10 kW to 30 kW, due to the fluctuations of illumination intensity for DG_1, DG_3, and wind speed for DG_6, DG_8 and DG_9, as shown in Fig. 4(a), while the active power outputs of DG_1, DG_3, DG_6, DG_8 and DG_9 are illustrated in Fig. 4(b).

Furthermore, the load demands also change over time and are scheduled as follows,

- $t = 3$ s: active loads decrease by 15% and reactive loads increase by 15%;
- $t = 6$ s: both active and reactive loads decrease by 15%;
- $t = 8$ s: both active and reactive loads increase by 25%,

where the fluctuations of total active and reactive loads are illustrated in Fig. 4(c).

A. Case 1: Reactive Power Sharing

In this case, the control laws I and laws II are used respectively, to investigate whether the control model achieves the proportional power sharing among controllable DGs, when both environmental conditions and the load demands change at the same time.

First, the control laws I are utilized, according to the topology of communication network 1 shown in Fig. 1, Agent_1, Agent_2, Agent_3, Agent_4 and Agent_5 collect the information of reactive power outputs of controllable DGs to which they connect, $Q_i, i = 2, 4, 5, 7, 10$, respectively. After that, the reactive power ratios can be calculated and are exchanged among neighboring agents. Receiving the information of neighbors, the reference reactive power ratios, $\beta_i^{\mathrm{ref}}, i = 1, 2, 3, 4, 5$ are calculated according to control laws from (21) to (25), respectively. Thereafter, the reference reactive power outputs for controllable DGs, $Q_i^{\mathrm{ref}}, i = 2, 4, 5, 7, 10$ are obtained in terms of equations

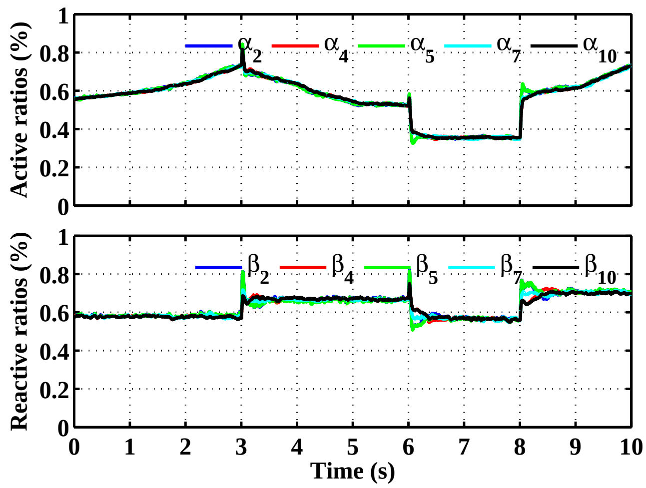

(a) t_d = 0.08 s.

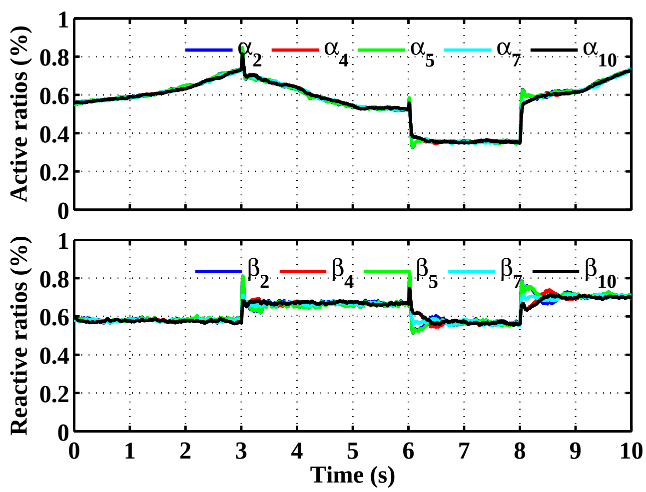

(b) t_d = 0.1 s.

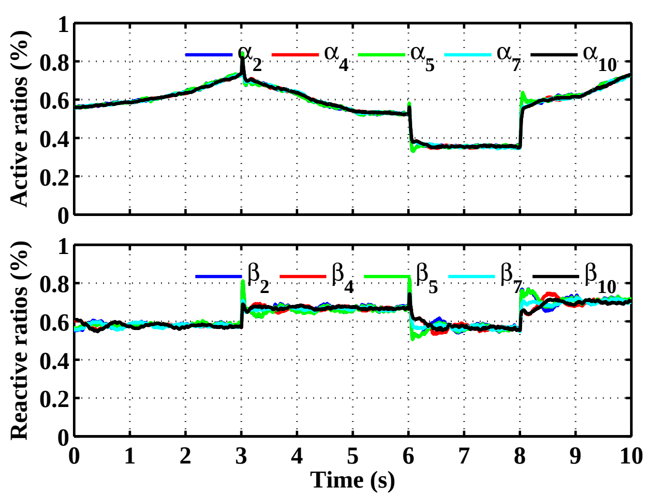

(c) t_d = 0.12 s.

Fig. 7. Case 2: Simulation results under the control laws I when time delays t_d are involved, and both the environmental conditions and load demands change over time.

from (26) to (30), respectively.

Consequently, the reference reactive power outputs are compared with measured values, respectively. Moreover, the errors between references and measured values are fed to PI controllers, and the produced reactive power correction terms, $\delta Q_i, i = 1, 2, 3, 4, 5$ are sent to controllable DGs to regulate their reactive power outputs, allowing reactive power outputs converge to references gradually. Meanwhile, the reactive power ratios also approach references, respectively. Therefore, it can be found in Fig. 5(a) and Fig. 5(b) that the load demands are shared proportionately among controllable DGs, and power ratios stay the same regardless of variations in load demands.

In addition, it can be found in Fig. 1 that each agent exchanges the information with two neighbors in network 1. However, in network 2, Agent$_1$, Agent$_3$ and Agent$_4$ simply have one neighbor, and Agent$_5$ exchanges the information with three neighbors. On the other hand, according to the discussion in Section II B, many possible communication networks can be considered for a given MG, and each communication network possesses a set of control laws, moreover, the control laws derived from different communication networks are supposed to have the similar performance. In order to verify the feasibility of the communication network 2, the control laws II derived from communication network 2 are used, and the simulation results are drawn in Fig. 6, which are similar to those that obtained under the control laws I. Therefore, the simulation results are consistent with the discussion. However, how the topology affects the performance of the control model requires further investigation.

B. Case 2: Impacts of Time Delays

As is known, the time delays on the communication network may possibly result in performance deterioration or even instability of the MG system. Therefore, in order to examine the impacts of time delays, the control laws I are adopted, and fixed time delays are taken into account on the communication among agents at each sample time, when both active power outputs of intermittent DGs and load demands fluctuate simultaneously.

Furthermore, Fig. 7 displays the effects of communication delays on reactive power sharing performance, when three fixed time delays t_d are employed, namely t_d = 0.08, 0.1 and 0.12 s, respectively. From Fig. 7(a) and Fig. 7(b), it can be seen that the control model is robust with time delays of t_d = 0.08 and 0.1 s. However, comparing with Fig. 7(a) and Fig. 7(c), it can be observed that the system dynamic has slowed down, when longer time delays are involved, because the control laws are calculated using lagged information from neighboring agents, when time delays are involved.

C. Case 3: Plug and Play Capability

In this case, both the active power outputs of intermittent DGs and load demands change at the same time, and the control laws II for communication network 2 are utilized. Note that controllable DGs have already reached the steady states before the plug out of controllable DG$_5$. At t = 4 s, the controllable DG$_5$ is disconnected from the MG, and

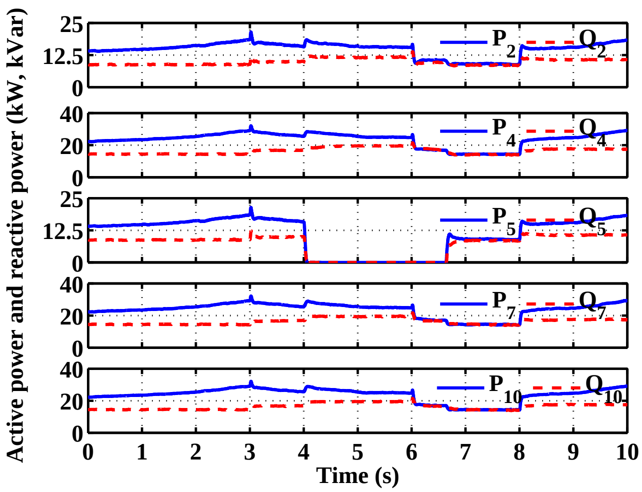

(a) power outputs of controllable DGs.

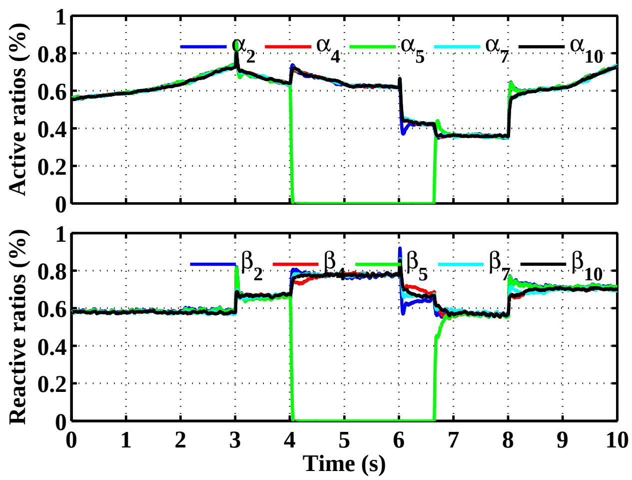

(b) power ratios of controllable DGs.

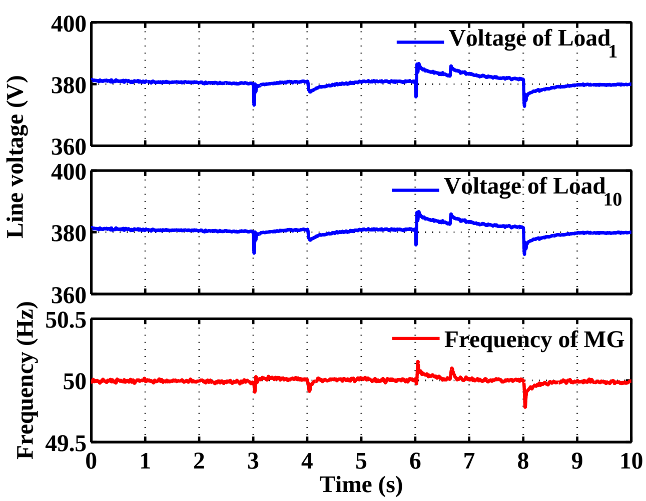

(c) frequency and line voltages in the MG.

Fig. 8. Case 3: Simulation results under the plug and play of DG_5, when the control laws II are used, and the active power outputs of intermittent DGs and load demands fluctuate simultaneously.

corresponding $Agent_3$, and associated communication links are excluded from the communication network, as shown in Fig. 9. With the consideration of power mismatch under new situations, the remaining controllable DGs produce more power to compensate for the amount of power previously generated by DG_5, as shown in Fig. 8(a). Therefore, there are increases in power ratios with increasing power outputs, while those of DG_5 drop to zero during the plug out, as illustrated in Fig. 8(b), because the information of DG_5 is not available to the agents.

Moreover, it can be found from Fig. 9 that the plug out of $Agent_3$ does not hinder the graphical connectivity of the communication network. In other words, there are no isolated agents on the communication network, and the remaining communication network allows communication among agents, which is identified as an essential ingredient for reactive power sharing. Therefore, after the plug out of DG_5 and $Agent_3$, agents calculate reference reactive power ratios, in terms of concrete formulas of control laws in (6), which take the following forms

$$\beta_1^{\text{ref}} = \frac{3}{4}\beta_1 + \frac{1}{4}\beta_5, \tag{38}$$

$$\beta_2^{\text{ref}} = \frac{3}{4}\beta_2 + \frac{1}{4}\beta_5, \tag{39}$$

$$\beta_3^{\text{ref}} = \beta_3, \tag{40}$$

$$\beta_4^{\text{ref}} = \frac{3}{4}\beta_4 + \frac{1}{4}\beta_5, \tag{41}$$

$$\beta_5^{\text{ref}} = \frac{1}{4}\beta_1 + \frac{1}{4}\beta_2 + \frac{1}{4}\beta_4 + \frac{1}{4}\beta_5. \tag{42}$$

Thereafter, the reference reactive power outputs for controllable DGs can be calculated, in terms of the equations from (26) to (30). Finally, according to the references, agents adjust the reactive power outputs of controllable DGs, for the purpose of proportional reactive power sharing, and the power ratios are illustrated in Fig. 8(b).

Furthermore, at $t = 6$ s, the synchronization strategy is activated and the seamless plug in of DG_5 into the MG is achieved at $t = 6.5$ s, and the corresponding $Agent_3$ is reconnected to the communication network simultaneously. Similarly, in terms of (6), the control laws under the new situations are derived and implemented, which are identical to the control laws II. Moreover, it can be seen in Fig. 8(b) that despite plug out and plug in operations of DG_5 and $Agent_3$, the control laws quickly drive the power ratios to equal values. That is, the capability of the control model to meet the requirement of plug and play operation is verified.

On the other hand, Fig. 8(c) shows that frequency stays around nominal value, namely 50 Hz, in all situations, and line voltages at the head and the tail of the bus, which are represented by voltages of $Load_1$ and $Load_{10}$ respectively, are still in a normal range, as shown in Fig. 8(c), even if large fluctuations in load demands occur at $t = 3$ s, 6 s and 8 s, which satisfy IEEE Standard 1547 requirements [42].

VI. Conclusion

Regarding to reactive power sharing in an islanded droop-controlled MG, an MAS based two-layer control model is

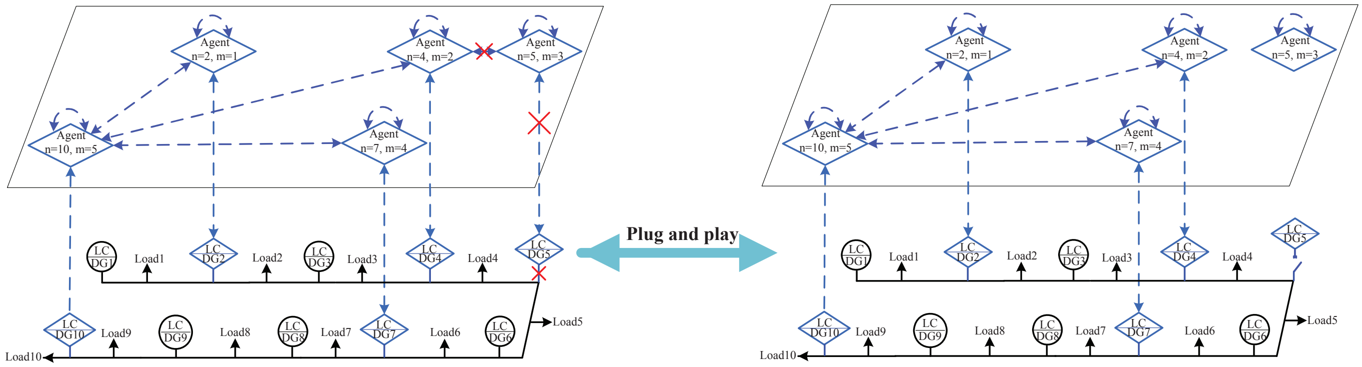

Fig. 9. The plug and play of DG_5 and $Agent_3$.

proposed in this paper. The bottom layer of the control model is the electrical distribution MG, while the top layer is a communication network composed of agents. In the control model, agents collect the information of reactive power ratios locally, and then agents process the acquired information in terms of the control laws. Moreover, a theorem is demonstrated for deriving the distributed control laws from a given communication network. Therefore, the reference reactive power outputs for controllable DGs can be calculated conveniently. Thereafter, agents send references to controllable DGs they connect to, to regulate their reactive power outputs, with the aim of proportional power sharing.

In order to evaluate the performance of the control model, three simulations cases are carried out and the results show that all controllable DGs have almost the same reactive power ratios, when the control laws are utilized, i.e., the proportional power sharing is achieved. Furthermore, the plug out and plug in behaviors of the controllable DG almost do not affect the power sharing performance, due to the plug and play capability of the control model.

For our future work, how the package loss, failure and topology affect the performance of the control model is also an open question for further investigation.

Acknowledgment

This work is supported by the National Natural Science Foundation of China (Grant No. 51177177 & No. 61105125) and National "111" Project (Grant No. B08036).

References

[1] D. Abbott, "Keeping the energy debate clean: How do we supply the world's energy needs?" *Proc. IEEE*, vol. 98, no. 1, pp. 42–66, 2010.
[2] R. H. Lasseter, "Smart distribution: Coupled microgrids," *Proc. IEEE*, vol. 99, no. 6, pp. 1074–1082, 2011.
[3] K. Ubilla, G. A. Jiménez-Estévez, R. Hernádez, L. Reyes-Chamorro, C. H. Irigoyen, B. Severino, and R. Palma-Behnke, "Smart microgrids as a solution for rural electrification: Ensuring long-term sustainability through cadastre and business models," *IEEE Trans. Sustainable Energy*, vol. 5, no. 4, pp. 1310–1318, 2014.
[4] D. Olivares, A. Mehrizi-Sani, A. Etemadi, C. Cañizares, R. Iravani, M. Kazerani, A. Hajimiragha, O. Gomis-Bellmunt, M. Saeedifard, R. Palma-Behnke, G. Jiménez-Estévez, and N. Hatziargyriou, "Trends in microgrid control," *IEEE Trans. Smart Grid*, vol. 5, no. 4, pp. 1905–1919, 2014.
[5] M. Yazdanian and A. Mehrizi-Sani, "Distributed control techniques in microgrids," *IEEE Trans. Smart Grid*, vol. 5, no. 6, pp. 2901–2909, 2014.
[6] H. Xin, Z. Qu, J. Seuss, and A. Maknouninejad, "A self-organizing strategy for power flow control of photovoltaic generators in a distribution network," *IEEE Trans. Power Syst*, vol. 26, no. 3, pp. 1462–1473, 2011.
[7] H. Xin, Z. Lu, Y. Liu, and D. Gan, "A center-free control strategy for the coordination of multiple photovoltaic generators," *IEEE Trans. Smart Grid*, vol. 5, no. 3, pp. 1262–1269, 2014.
[8] H. Xin, M. Zhang, J. Seuss, Z. Wang, and D. Gan, "A real-time power allocation algorithm and its communication optimization for geographically dispersed energy storage systems," *IEEE Trans. Power Syst*, vol. 28, no. 4, pp. 4732–4741, 2013.
[9] W. Liu, W. Gu, W. Sheng, X. Meng, Z. Wu, and W. Chen, "Decentralized multi-agent system-based cooperative frequency control for autonomous microgrids with communication constraints," *IEEE Trans. Sustainable Energy*, vol. 5, no. 2, pp. 446–456, 2014.
[10] W. Gu, W. Liu, J. Zhu, B. Zhao, Z. Wu, Z. Luo, and J. Yu, "Adaptive decentralized under-frequency load shedding for islanded smart distribution networks," *IEEE Trans. Sustainable Energy*, vol. 5, no. 3, pp. 886–895, 2014.
[11] A. Bidram, A. Davoudi, F. L. Lewis, and Z. Qu, "Secondary control of microgrids based on distributed cooperative control of multi-agent systems," *IET Generation Transmission & Distribution*, vol. 7, no. 8, pp. 822–831, 2013.
[12] A. Bidram, A. Davoudi, F. L. Lewis, and J. M. Guerrero, "Distributed cooperative secondary control of microgrids using feedback linearization," *IEEE Trans. Power Syst.*, vol. 28, no. 3, pp. 3462–3470, 2013.
[13] T. Morstyn, B. Hredzak, and V. G. Agelidis, "Distributed cooperative control of microgrid storage," *IEEE Trans. Power Syst.*, vol. 30, no. 5, pp. 2780–2789, 2015.
[14] M. Mao, P. Jin, N. D. Hatziargyriou, and L. Chang, "Multiagent-based hybrid energy management system for microgrids," *IEEE Trans. Sustainable Energy*, vol. 5, no. 3, pp. 938–946, 2014.
[15] Q. Li, F. Chen, M. Chen, J. M. Guerrero, and D. Abbott, "Agent-based decentralized control method for islanded microgrids," *IEEE Trans. Smart Grid*, vol. 7, no. 2, pp. 637–648, 2016.
[16] A. Bidram and A. Davoudi, "Hierarchical structure of microgrids control system," *IEEE Trans. Smart Grid*, vol. 3, no. 4, pp. 1963–1976, 2012.
[17] J. M. Guerrero, M. Chandorkar, T.-L. Lee, and P. C. Loch, "Advanced control architectures for intelligent microgrids—Part I: Decentralized and hierarchical control," *IEEE Trans. Ind. Electron.*, vol. 60, no. 4, pp. 1254–1262, 2013.
[18] J. M. Guerrero, L. G. d. Vicuña, J. Matas, M. Castilla, and J. Miret, "Output impedance design of parallel-connected ups inverters with wireless load-sharing control," *IEEE Trans. Ind. Electron.*, vol. 52, no. 4, pp. 1126–1135, 2005.
[19] J. M. Guerrero, J. Matas, L. G. d. Vicuña, M. Castilla, and J. Miret, "Wireless-control strategy for parallel operation of distributed-generation inverters," *IEEE Trans. Ind. Electron.*, vol. 53, no. 5, pp. 1161–1169, 2006.
[20] Y. A.-R. I. Mohamed and E. F. El-Saadany, "Adaptive decentralized droop controller to preserve power sharing stability of paralleled inverters in distributed generation microgrids," *IEEE Trans. Power Electron.*, vol. 23, no. 6, pp. 2806–2816, 2008.
[21] M. M. A. Abdelaziz, H. E. Farag, and E. F. El-Saadany, "Optimum droop parameter settings of islanded microgrids with renewable energy

resources," *IEEE Trans. Sustainable Energy*, vol. 5, no. 2, pp. 434–446, 2014.

[22] Y. Zhu, F. Zhuo, F. Wang, B. Liu, and Y. Zhao, "A wireless load sharing strategy for islanded microgrid based on feeder current sensing," *IEEE Trans. Power Electron.*, vol. 30, no. 12, pp. 6706–6718, 2015.

[23] Q. Shafiee, J. M. Guerrero, and J. C. Vasquez, "Distributed secondary control for islanded microgrids—A novel approach," *IEEE Trans. Power Electron.*, vol. 29, no. 2, pp. 1018–1031, 2014.

[24] Q. Shafiee, C. Stefanović, T. Dragičević, P. Popovski, J. C. Vasquez, and J. M. Guerrero, "Robust networked control scheme for distributed secondary control of islanded microgrids," *IEEE Trans. Ind. Electron.*, vol. 61, no. 10, pp. 5363–5374, 2014.

[25] Q. Shafiee, V. Nasirian, J. M. Guerrero, F. L. Lewis, and A. Davoudi, "Team-oriented adaptive droop control for autonomous AC microgrids," in *IEEE 40th Annual Industrial Electronics Society Conference*, 2014, pp. 1861–1867.

[26] V. Nasirian, Q. Shafiee, J. M. Guerrero, F. L. Lewis, and A. Davoudi, "Droop-free distributed control for AC microgrids," *IEEE Trans. Power Electron.*, vol. 31, no. 2, pp. 1600–1615, 2016.

[27] A. Bidram, A. Davoudi, and F. L. Lewis, "A multi-objective distributed control framework for islanded AC microgrids," *IEEE Trans. Ind. Informat.*, vol. 10, no. 3, pp. 1785–1798, 2014.

[28] F. Guo, C. Wen, J. Mao, and Y.-D. Song, "Distributed secondary voltage and frequency restoration control of droop-controlled inverter-based microgrids," *IEEE Trans. Ind. Electron.*, vol. 62, no. 7, pp. 4355–4365, 2015.

[29] J. W. Simpson-Porco, Q. Shafiee, F. Dörfler, J. C. Vasquez, J. M. Guerrero, and F. Bullo, "Secondary frequency and voltage control of islanded microgrids via distributed averaging," *IEEE Trans. Ind. Electron.*, vol. 62, no. 11, pp. 7025–7038, 2015.

[30] M. A. Mahmud, M. J. Hossain, H. R. Pota, and A. M. T. Oo, "Robust nonlinear distributed controller design for active and reactive power sharing in islanded microgrids," *IEEE Trans. Energy Convers.*, vol. 29, no. 4, pp. 893–901, 2014.

[31] J. Schiffer, T. Seel, J. Raisch, and T. Sezi, "Voltage stability and reactive power sharing in inverter-based microgrids with consensus-based distributed voltage control," *IEEE TRANSACTIONS ON CONTROL SYSTEMS TECHNOLOGY*, vol. 24, no. 1, pp. 96–108, 2016.

[32] H. Han, Y. Liu, Y. Sun, M. Su, and J. M. Guerrero, "An improved droop control strategy for reactive power sharing in islanded microgrid," *IEEE Trans. Power Electron.*, vol. 30, no. 6, pp. 3133–3140, 2015.

[33] L.-Y. Lu and C.-C. Chu, "Consensus-based droop control synthesis for multiple DICs in isolated micro-grids," *IEEE Trans. Power Syst*, vol. 30, no. 5, pp. 2243–2255, 2015.

[34] H. Zhang, S. Kim, Q. Sun, and J. Zhou, "Distributed adaptive virtual impedance control for accurate reactive power sharing based on consensus control in microgrids," *IEEE Trans. Smart Grid*, 2015, DOI: 10.1109/TSG.2015.2506760.

[35] T. Dragičević, X. Lu, J. C. Vasquez, and J. M. Guerrero, "DC microgrids—Part I: A review of control strategies and stabilization techniques," *IEEE Trans. Power Electron.*, vol. 31, no. 7, pp. 4876–4888, 2016.

[36] S. Anand, B. G. Fernandes, and J. M. Guerrero, "Distributed control to ensure proportional load sharing and improve voltage regulation in low-voltage DC microgrids," *IEEE Trans. Power Electron.*, vol. 28, no. 4, pp. 1900–1914, 2013.

[37] V. Nasirian, S. Moayedi, A. Davoudi, and F. L. Lewis, "Distributed cooperative control of DC microgrids," *IEEE Trans. Power Electron.*, vol. 30, no. 4, pp. 2288–2303, 2015.

[38] L. Meng, T. Dragičević, J. Roldán-Pérez, J. C. Vasquez, and J. M. Guerrero, "Modeling and sensitivity study of consensus algorithm-based distributed hierarchical control for DC microgrids," *IEEE Trans. Smart Grid*, 2015, DOI: 10.1109/TSG.2015.2422714.

[39] A. A. Hamad, M. A. Azzouz, and E. F. El-Saadany, "Multiagent supervisory control for power management in DC microgrids," *IEEE Trans. Smart Grid*, vol. 7, no. 2, pp. 1057–1067, 2016.

[40] Q. Kang, M. Zhou, J. An, and Q. Wu, "Swarm intelligence approaches to optimal power flow problem with distributed generator failures in power networks," *IEEE Trans. Autom. Sci. Eng*, vol. 10, no. 2, pp. 343–353, 2013.

[41] J. M. Guerrero, J. C. Vasquez, J. Matas, L. G. d. Vicuña, and M. Castilla, "Hierarchical control of droop-controlled AC and DC microgrids—A general approach toward standardization," *IEEE Trans. Ind. Electron.*, vol. 58, no. 1, pp. 158–172, 2011.

[42] T. S. Basso and R. DeBlasio, "IEEE 1547 series of standards: Interconnection issues," *IEEE Trans. Power Electron.*, vol. 19, no. 5, pp. 1159–1162, 2004.

Feixiong Chen received the B.S. degree in electrical engineering from Chongqing University of Technology, Chongqing, China, in 2012. He is currently pursuing the Ph.D. degree with the School of Electrical Engineering, Chongqing University, Chongqing, China.

His current research interests include multiagent systems and optimization of microgrids.

Minyou Chen (M'05−SM'14) received the M.Sc. degree in control theory and engineering from Chongqing University, China, in 1987, and the Ph.D. degree in control engineering from the University of Sheffield, Sheffield, U.K., in 1998.

He is currently a Full Professor with Chongqing University. His current research interests include intelligent modeling and control, multiobjective optimization, microgrid control, and state monitoring in power distribution systems. He has authored or co-authored over 180 papers.

Qiang Li received the B.S. degree in electrical engineering from Sichuan Institute of Technology, China, in 2001, the M.S. degree in control theory and engineering from Chongqing University, China, in 2004, and the Ph.D. degree in electrical engineering from Zhejiang University, China, in 2009.

He was a Postdoctoral Fellow with Chongqing University from 2009 to 2012, and a Visiting Postdoctoral Scholar with the University of Adelaide, Adelaide, SA, Australia, from 2011 to 2012. From 2014 to 2015, he was a Visiting Postdoctoral Scholar with Boston University, Boston, MA, USA. He is currently an Associate Professor with Chongqing University. His current research interests include networked control systems, optimization of microgrids, evolutionary dynamics, and quantum games.

Kaikai Meng received the B.S. degree in applied physics from Chongqing University, Chongqing, China, in 2012, the M.S. degree in electrical engineering from School of Electrical Engineering, Chongqing University, Chongqing, China, in 2015.

She is currently with Fuzhou Power Supply Company of State Grid Fujian Electric Power Company, Fujian, China, where she is engaged with the operation and control of power systems.

Josep M. Guerrero (S'01–M'04–SM'08–F'15) received the B.S. degree in telecommunications engineering, the M.S. degree in electronics engineering, and the Ph.D. degree in power electronics from the Technical University of Catalonia, Barcelona, in 1997, 2000 and 2003, respectively. Since 2011, he has been a Full Professor with the Department of Energy Technology, Aalborg University, Denmark, where he is responsible for the Microgrid Research Program. From 2012 he is a guest Professor at the Chinese Academy of Science and the Nanjing University of Aeronautics and Astronautics; from 2014 he is chair Professor in Shandong University; and from 2015 he is a distinguished guest Professor in Hunan University.

His research interests are oriented to different microgrid aspects, including power electronics, distributed energy-storage systems, hierarchical and cooperative control, energy management systems, and optimization of microgrids and islanded microgrids; recently specially focused on maritime microgrids for electrical ships, vessels, ferries and seaports. Prof. Guerrero is an Associate Editor for the IEEE Transactions on Power Electronics, the IEEE Transactions on Industrial Electronics, and the IEEE Industrial Electronics Magazine, and an Editor for the IEEE Transactions on Smart Grid and IEEE Transactions on Energy Conversion. He has been Guest Editor of the IEEE Transactions on Power Electronics Special Issues: Power Electronics for Wind Energy Conversion and Power Electronics for Microgrids; the IEEE Transactions on Industrial Electronics Special Sections: Uninterruptible Power Supplies systems, Renewable Energy Systems, Distributed Generation and Microgrids, and Industrial Applications and Implementation Issues of the Kalman Filter; and the IEEE Transactions on Smart Grid Special Issue on Smart DC Distribution Systems. He was the chair of the Renewable Energy Systems Technical Committee of the IEEE Industrial Electronics Society. He received the best paper award of the IEEE Transactions on Energy Conversion for the period 2014-2015. In 2014 and 2015 he was awarded by Thomson Reuters as Highly Cited Researcher, and in 2015 he was elevated to IEEE Fellow for his contributions on distributed power systems and microgrids.

Derek Abbott (M'85–SM'99–F'05) was born in South Kensington, London, U.K., in 1960. He received the B.Sc. (honors) degree in physics from Loughborough University, Leicestershire, U.K., in 1982 and the Ph.D. degree in electrical and electronic engineering from The University of Adelaide, Adelaide, S.A., Australia, in 1995, under K. Eshraghian and B. R. Davis. From 1978 to 1986, he was a Research Engineer at the GEC Hirst Research Centre, London, U.K. From 1986 to 1987, he was a VLSI Design Engineer at Austek Microsystems, Australia. Since 1987, he has been with The University of Adelaide, where he is presently a full Professor with the School of Electrical and Electronic Engineering. He holds over 800 publications/patents and has been an invited speaker at over 100 institutions. He coedited *Quantum Aspects of Life* (London, U.K.: Imperial College Press, 2008), coauthored *Stochastic Resonance,* (Cambridge, U.K.: Cambridge Univ. Press, 2008), and coauthored *Terahertz Imaging for Biomedical Applications,* (New York, NY, USA: Springer-Verlag, 2012). His interest is in the area of multidisciplinary physics and electronic engineering applied to complex systems. His research programs span a number of areas including networks, game theory, energy policy, stochastics, and biophotonics. Prof. Abbott is a Fellow of the Institute of Physics (IOP) and Fellow of the Institute of Electrical & Electronic Engineers. He has won a number of awards including the South Australian Tall Poppy Award for Science (2004), an Australian Research Council (ARC) Future Fellowship (2012), and the David Dewhurst Medal, Australia (2015). Prof. Abbott has served as an Editor and/or Guest Editor for a number of journals including the IEEE Journal of Solid-State Circuits, *Journal of Optics B, Microelectronics Journal, PLOSONE,* Proceedings of the IEEE, and the IEEE Photonics Journal. He is currently on the editorial boards of Nature's *Scientific Reports*, *Royal Society Open Science*, and IEEE Access.